RESERVOIR POROSITY DETERMINATION FROM 3D SEISMIC DATA - APPLICATION OF TWO MACHINE LEARNING TECHNIQUES

ANDISHEH ALIMORADI[1], ALI MORADZADEH[1] and MOHAMMAD REZA BAKHTIARI[2,3]

[1] *Department of Mining, Petroleum and Geophysics Engineering, Shahrood University of Technology, Shahrood, Iran. andisheh.alimoradi@yahoo.com*
[2] *Department of Petroleum Engineering, Amir Kabir University of Technology (Tehran Polytechnic), Tehran, Iran.*
[3] *National Iranian Oil Company, Exploration Directorate, Tehran, Iran.*

(Received February 1, 2012; revised version accepted September 9, 2012)

ABSTRACT

Alimoradi, A., Moradzadeh, A. and Bakhtiari, M.R., 2012. Reservoir porosity determination from 3D seismic data - application of two machine learning techniques. *Journal of Seismic Exploration*, 21: 323-345.

This paper proposes a method for solving 3D seismic data inversion problems for prediction of porosity in hydrocarbon reservoirs. An actual carbonate oil field in the south-western part of Iran was selected for this study. Taking real geological conditions into account, different synthetic models of reservoir were constructed for a range of viable porosity values. Seismic surveying was performed next on these models. From seismic response of the synthetic models, a large number of seismic attributes were identified as candidates for porosity estimation. Classes of attributes such as energy, instantaneous, and frequency attributes were included amongst others. Applying sensitivity analysis, the two most significant attributes were determined as Envelope Weighted Phase and Envelope Weighted Frequency, which were subsequently used in our machine learning algorithms. In particular, we used feed-forward artificial neural networks (FNN) and support vector regression machines (SVR) to develop relationships between the known synthetic attributes and synthetic porosity values in a given setting. The FNN consists of six neurons in a single hidden layer and the SVR method uses a Gaussian radial basis function. Compared with real values from the well data, we observed that SVM outperforms FNN due to its better handling of noise and model complexity.

KEY WORDS: seismic inversion, seismic attributes, synthetic data, feed forward neural network, support vector machine.

0963-0651/12/$5.00

INTRODUCTION

Reservoir porosity is one of the fundamental rock properties which relates to the amount of fluid contained in a reservoir and its ability to flow when subjected to applied pressure gradients. This property has a significant impact on petroleum fields operations and reservoir management.

Since well logging tools became available, calculating formation porosity from geophysical well logs has been practiced. In many situations, there may exist relationships between the value of porosity and acoustic transit time (Δt); but such correlations are usually empirically derived for a given formation in a given area. One of the first relationships to determine porosity from sonic transit time was proposed in 1958 (Wyllie et al., 1958). This equation is almost used to quantifying porosity in consolidated sandstones and carbonates with intergranular porosity. Better results can be found using $Cp = \Delta tsh/100$, which was introduced later. Raymer investigated an empirical sonic porosity transform based on comparison of transit times with core porosities and porosities derived from other logs (Raymer et al., 1980). Other petrophysicists worked on equations which relate sonic transit time (Δt) and porosity (φ) better than the Wyllie Time Average equation.

These calculations assume a linear or modeled nonlinear relationship between porosity and density log responses. Log analysis in a large field-scale study can be quite labor intensive and time consuming and therefore, expensive. This problem becomes more pronounced when the formation being studied is known to be a complex system. For more complicated relationships found in many oil field problems, such simple tools often do not provide adequate solutions. To solve this problem, scientists have focused on Artificial Intelligence as a nonlinear and non-parametric tool in well log analysis. Different types of artificial neural networks (ANN) and fuzzy logic (FL) have been used for reservoir characterization and also for well log interpretation (Pezeshk et al., 1996; Jang et al., 1997; Batyrshin et al., 2002; Nikravesh et al., 2003). One of the best results presented in 1996, obtained porosity in a sandstone oil field using gamma ray, deep induction and bulk density logs and the three layer feed forward back propagation artificial neural network (Mohaghegh et al., 1996). Mohaghegh also introduced a neural network approach which can find the relationship between neutron logs and the values of porosity parameter (Mohaghegh et al., 1999). Lim suggested an intelligent technique using fuzzy logic and neural network to determine porosity from conventional well logs (Lim, 2005). Batyrshin described a methodology based on the use of hybrid methods, such as principal component and factor analysis, fuzzy classification and evolutionary optimizations for analysis of well logs and for qualitative pore structure classification in carbonate formations (Batyrshin et al., 2005).

Although reservoir porosity can be derived reliably from core samples or well-log measurements, this property varies laterally from one well to another. Normally, it is very difficult to predict the reservoir properties away from the wells, especially near the edge of an oil field. Seismic data, particularly 3D surveys, contain valuable information about the lateral variation of reservoir properties. When there are wells inside the seismic coverage, it is natural to infer the reservoir property between the wells by interpreting the seismic data and using the reservoir property at well locations as spatial control points. In 1998, Lawrence could predict fractures in a carbonate reservoir using the combination of impedance and coherence attributes (Lawrence, 1998). Leu found a statistical regression between wave amplitude and velocity with porosity values from logs (Leu et al., 1999). Others used seismic facies analysis to investigate the lateral changes of porosity (Edalat and Siahkoohi, 2007). Assuming that there exists a functional or statistical relationship between the seismic data and the reservoir property, ANNs can be applied to establish a model of the relationship using the training sample set. This model can then be used to predict the reservoir properties away from the wells (An and Moon, 1993; An, 1994). An proposed the ANN method to predict porosity values in one Canadian oil field using seismic wave amplitude (An et al., 1997). Malvic and Prskalo (2007) suggested a back propagation artificial neural network to relate the values of amplitude, phase and frequency attributes to the values of porosity parameter.

This paper suggests an intelligent technique for reservoir characterization using artificial neural network and support vector machine to determine reservoir porosity from seismic attributes. A real example of a reservoir characterization project in south western part of Iran using these approaches is given. Since data obtained from the oil field being studied were not adequate for ANN and SVM modeling process, we decided generating synthetic data, finding the proper network, and checking the network with the data of abovementioned oil field.

METHODOLOGY

Site Geology

One of the Iranian carbonate oil field which is located in the south-western part of Iran was selected. This field consists of all of the necessary data for this study including 3D seismic data and well data (cores and logs). There are also two wells drilled in this field. Both of these wells contain hydrocarbon in Sarvak level (one of the famous hydrocarbon zones in Iranian carbonate oil fields) at the depth of 2850 meters. The thickness of the reservoir is about 200 meters. Since the data of well 1 are so noisy and incomplete, we decided to implement well 2 in this study. Geological investigations illustrate that the

reservoir through this well (well 2) consists of pure limestone. The values of porosity obtained from well log measurements are shown in Fig. 1.

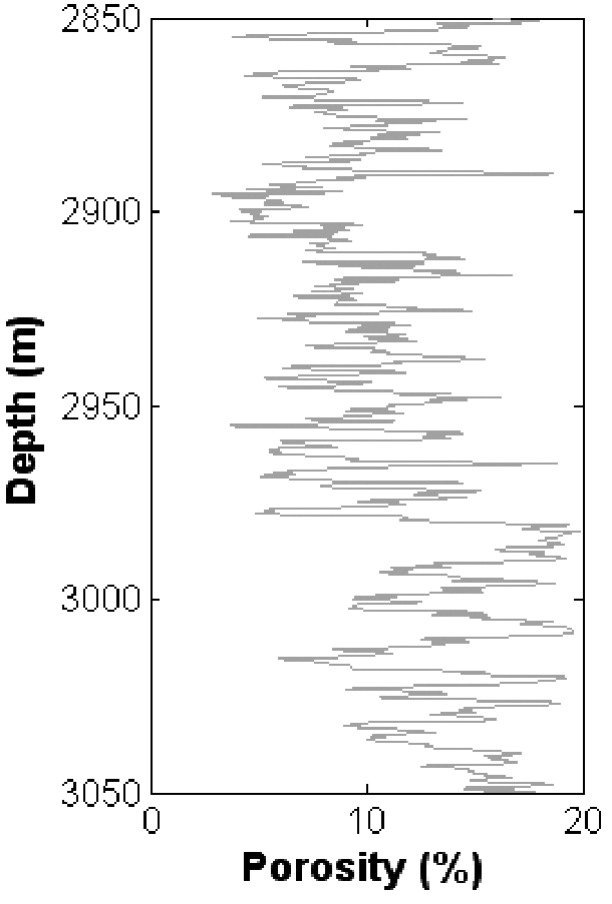

Fig. 1. Values of porosity in well 2 through the reservoir zone.

Seismic Data Acquisition

The proposed methodology of this paper will be explained using a realistic example. A 3D seismic survey has been performed over this field. Fig. 2 illustrates the seismic line which passes both wells. Since OpendTect is one of the most powerful packages in seismic data interpretation, the application of this software was considered for seismic attribute extraction. As previously mentioned, the data of well 1 are not suitable for analysis; therefore it is inevitable to work on the data of well 2 only. According to limited resolution of seismic survey which leads to the limited number of data points in discrete well analysis, it is necessary to generate adequate synthetic data.

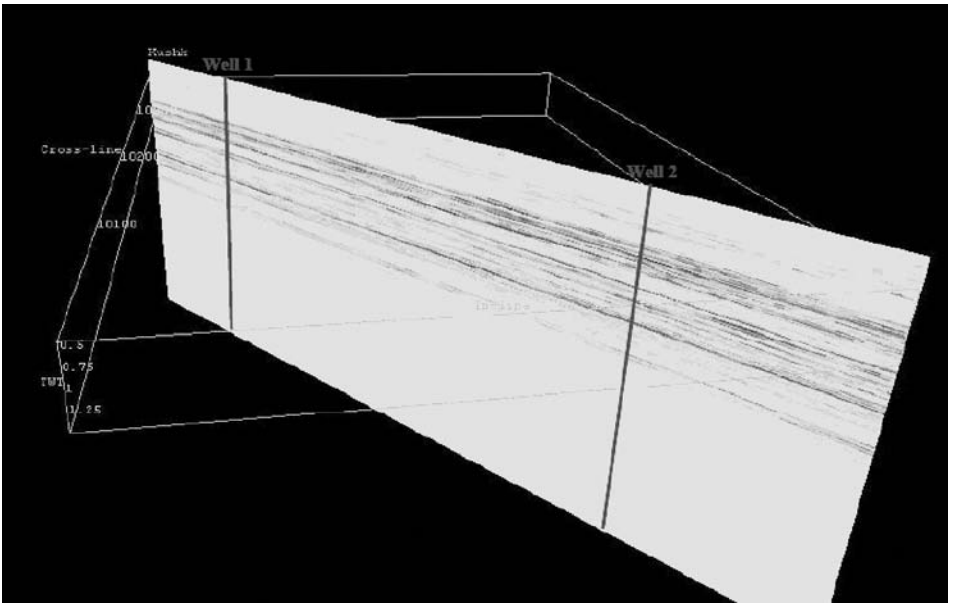

Fig. 2. Seismic line over wells 1 and 2 (dGB Earth Sciences, 2008).

Forward modeling was done to simulate a reservoir level in Sarvak zone for well 2 using modified Gassmann rock physics equation (Alimoradi et al., 2011):

$$\rho_{sat}V_{Psat}^2 = [(1 - \alpha K_{Gdry}/K_0)^2/\{(\varphi/K_{fl}) + (1-\varphi)/K_0 - (\alpha K_{Gdry}/K_0^2)\} + \alpha K_{Gdry} + (4/3)\mu] \quad . \tag{1}$$

In this equation:

ρ_{sat} = density of the saturated rock,
V_{Psat} = P-wave saturated rock velocity,
μ = rock shear modulus,
K_{Gdry} = dry rock effective bulk modulus from the Geertsema equation,
K_0 = bulk modulus of the mineral material making up the rock,
K_{fl} = effective bulk modulus of the pore fluid,
φ = porosity,
α = coefficient of pores sizes.

P-wave saturated rock velocity (V_{Psat}) data were generated by changing the values of φ and α. Other parameters in the Gassmann equation are considered to be constant (according to their real values in the reservoir). These parameters are: K_0 = 63 GPa, μ = 26 GPA, ρ = 2479 kg/m^3 and S_W = 0.3279, respectively. 45 data were generated in this way (Table 1) each called from model 101 to model 509. The first value in each model name refers to the values of porosity (0.1 to 0.5) and the third one refers to values of α (0.1 to 0.9). For example model 207 refers to the synthetic model which has a porosity of 0.2 and α of 0.7.

Table 1. 45 synthetic models generated using the modified Gassmann equation.

φ	K_{Gdry}	α	K_{dryNew}	V_P	Model	φ	K_{Gdry}	α	K_{dryNew}	V_P	Model
0.1	10.5	0.1	1.05	4573	101	0.2	5.73	0.1	0.573	4243	201
		0.2	2.1	4598	102			0.2	1.146	4263	202
		0.3	3.15	4624	103			0.3	1.719	4283	203
		0.4	4.2	4649	104			0.4	2.292	4302	204
		0.5	5.25	4675	105			0.5	2.865	4322	205
		0.6	6.3	4700	106			0.6	3.438	4341	206
		0.7	7.35	4726	107			0.7	4.011	4361	207
		0.8	8.4	4752	108			0.8	4.584	4380	208
		0.9	9.45	4778	109			0.9	5.157	4399	209
0.3	3.94	0.1	0.394	4101	301	0.4	3	0.1	0.3	4021	401
		0.2	0.788	4116	302			0.2	0.6	4034	402
		0.3	1.182	4132	303			0.3	0.9	4047	403
		0.4	1.576	4147	304			0.4	1.2	4059	404
		0.5	1.970	4163	305			0.5	1.5	4072	405
		0.6	2.364	4178	306			0.6	1.8	4084	406
		0.7	2.758	4193	307			0.7	2.1	4097	407
		0.8	3.152	4208	308			0.8	2.4	4109	408
		0.9	3.546	4224	309			0.9	2.7	4122	409
0.5	2.42	0.1	0.242	3971	501						
		0.2	0.484	3981	502						
		0.3	0.726	3992	503						
		0.4	0.968	4003	504						
		0.5	1.210	4013	505						
		0.6	1.452	4024	506						
		0.7	1.694	4034	507						
		0.8	1.936	4045	508						
		0.9	2.178	4056	509						

By preparing suitable codes in Seismic Unix forward modeling package, it is possible to construct the synthetic geological model. Fig. 3 shows the geological model for synthetic data 101. In this figure, "Zone L" illustrates the reservoir level. To make the model similar to the real reservoir, all levels above reservoir level exactly are considered with regard to their thickness and velocity. The objective is to perform seismic survey on the model and determine the seismic response of the model.

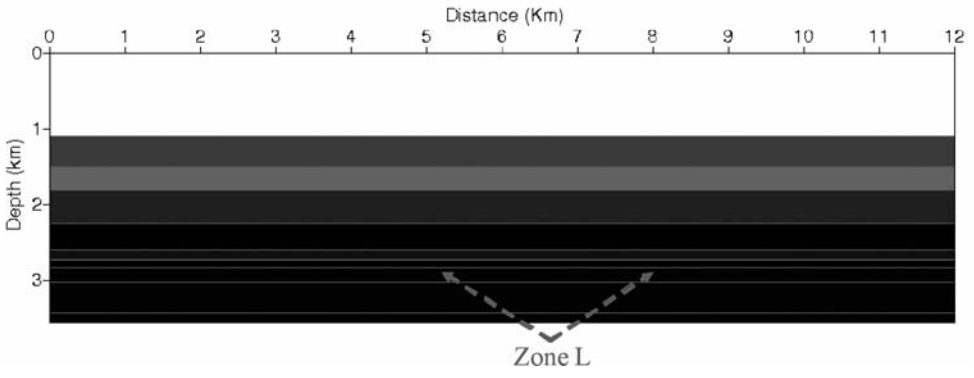

Fig. 3. Geological model of the reservoir constructed by Seismic Unix.

After constructing a geological model for each synthetic data, a pre-defined seismic survey (by writing suitable codes in the Seismic Unix package) is performed over constructed models in order to extract the seismic response of each model. The output of this step is then processed using ray tracing technique and stacked thoroughly to obtain the seismic section of the studied model. Therefore in 45 synthetic seismic sections each, one point to the specific porosity situation in the reservoir was extracted. Fig. 4 illustrates the stacked seismic section of model 101. These models can be used to extract attributes, make attribute analysis and study the effect of the changes in porosity on different attributes. Therefore it is possible to find related attributes with porosity parameter and model the relationship between those attributes and the values of porosity.

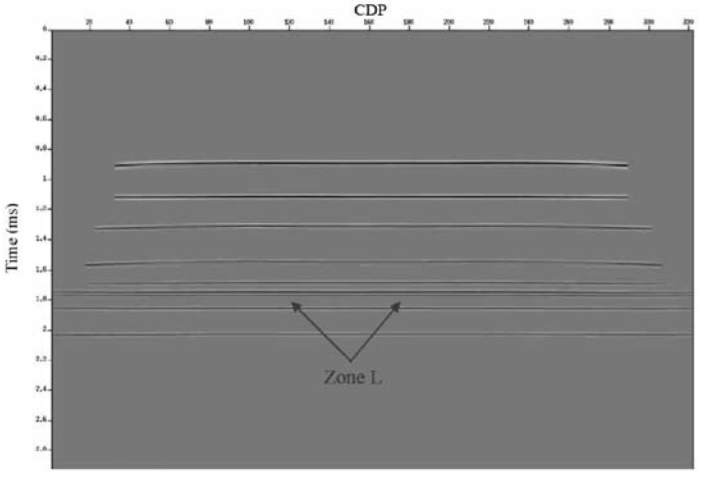

Fig. 4. The stacked seismic section of model 101.

Table 2. Values of 43 seismic attributes for model 101.

Energy/Energy	0.001516	Velocity Fan Filter	0.000213274
Energy/Sqrt	0.038938	Frequency/ Dominant Frequency	13.989712
Energy/Ln	−6.491552	Frequency/ Average Frequency	45.645275
Instantaneous/Amplitude	0.001748	Frequency/ Median Frequency	38.888885
Instantaneous/Phase	0.250555	Frequency/Average Frequency Squared	3006.6557
Instantaneous/Frequency	101.56539	Frequency/Maximum Spectral Amplitude	0.03902
Instantaneous/Hilbert	0.000433462	Frequency/Spectral Area Beyond Dominant Frequency	0.258528
Instantaneous/Amplitude/ 1st Derivative	0.205685	Frequency/Frequency Slope Fall	0.202982
Instantaneous/Amplitude/ 2nd Derivative	59.849281	Frequency/Absorption Quality Factor	14.671811
Instantaneous/Cosine Phase	0.968775	Spectral Decomp	3.73E-09
Instantaneous/Envelope Weighted Phase	0.224808	Event/Peakedness	0.000132157
Instantaneous/Envelope Weighted Frequency	109.31568	Event/Steepness	0.004993
Instantaneous/Phase acceleration	−3067.375	Event/Assymetry	0.597961
Instantaneous/Thin bed indicator	−7.75029	Volume Statistics Average	−0.013966
Instantaneous/Bandwidth	18.724953	Volume Statistics/Median	0.001047
Instantaneous/Q factor	−2.712033	Volume Statistics/Variance	0.001308
Convolve/Lowpass	0.001834	Volume Statistics/Min	−0.119581
Convolve/Laplacian	−0.000703483	Volume Statistics/Max	0.004804
Convolve/Prewitt	0.002109	Volume Statistics/Sum	−0.628459
Frequency Filter/LowPass	0.003497	Volume Statistics/ Norm Variance	4.014766
Frequency Filter/HighPass	−0.009834	Volume Statistics/RMS	0.038396
Frequency Filter/BandPass	−0.007492		

Attribute Extraction and Analysis

To investigate the effect of porosity changes on attribute values, the synthetic models classified into specific groups. Different values in each state were considered as a group (according to Table 1). Seismic attributes should be extracted in each group and attribute analysis performed over them. According to the proper capabilities of OpendTect software in seismic attribute analyzing and interpretation, this package was considered to extract attributes in our study.

OpendTect is an open source system for seismic data interpretation that interprets the huge volume of seismic data using attributes and new techniques of imaging. In this study, 43 different seismic attributes were extracted for all porosity models. Table 2 illustrates the values of these attributes for model 101.

In the next step, attributes were analyzed forming a correlation matrix. Using this matrix for all groups indicated that two attributes of *Envelope Weighted Phase* (EWP) and *Envelope Weighted Frequency* (EWF) have the highest correlation values with the values of porosity. EWP and EWF are an instantaneous phase and frequency which have been weighted with envelope over the specific time window. Instantaneous phase and frequency are two attributes which can be indicators of porous and fractured zones. Table 3 shows the values of correlation coefficient for these two attributes in all groups of porosity.

Table 3. Values of correlation coefficient for EWP and EWF.

Group	**R (EWP)**	**R (EWF)**
1 (Models 101 - 501)	−0.849	−0.859
2 (Models 102 - 502)	−0.804	−0.899
3 (Models 103 - 503)	−0.852	−0.936
4 (Models 104 - 504)	−0.874	−0.959
5 (Models 105 - 505)	−0.866	−0.949
6 (Models 106 - 506)	−0.864	−0.937
7 (Models 107 - 507)	−0.862	−0.924
8 (Models 108 - 508)	−0.812	−0.928
9 (Models 109 - 509)	−0.800	−0.925

Back-propagating Artificial Neural Networks (BANN)

Artificial neural networks (ANNs) are computational models based on human's understanding of cortical structure of the brain and cognition. Algorithmically, ANNs are parallel adaptive systems and therefore require training. Back-propagation is a powerful method of supervised learning that is developed after the seminal work by Paul Werbos and David E. Rumelhart in seventies and eighties (Demuth and Beale, 2002). Details of various methods of ANN design and training are beyond the scope of this paper and are explained elsewhere (see Hagan et al., 1996, for example); nevertheless a brief description of the terminology is provided here.

The structure of a neural network, in general, consists of an interconnected group of artificial neurons (simple processors that are connected to many other neurons). These processing units receive the information, apply some simple processing on them and pass them to other neurons. The flow of information creates a computational model for information processing. Each neuron is assigned a weight that is changed adaptively to improve the performance of the network based on pairs of external and internal signals (training information, input-output mapping). Practically, neural networks may be used in nonlinear statistical data modeling, system identification, extraction of complex relationships between inputs and outputs of a system, and for pattern recognition.

In addition to weight, each node (neuron) in the network is equipped with an activation function (or transfer function) that is part of the information processing unit of the neuron. The flow of information could be imagined from left to right, such that each neuron performs the processing on the data in parallel with other neurons in the layer. The response of the network is compared at the terminating layer with a set of desired outputs and the weights of the neurons are thus corrected following a training algorithm to minimize the output error. Issues with regards to the number of nodes per layer, number of layers, and the type of activation function that could be used are dealt with in the design of the architecture of the network. This is explained later on in this paper.

There are numerous methods of training of a neural network. Categorically these methods are grouped into three main classes: supervised learning, unsupervised learning, and reinforcement learning. In a supervised learning scheme, the network is provided with a set of examples in the input-output space: $(x,y), x \in X, y \in Y$ and the goal of the training process is to find function f in a set of valid functions that could match the input/output pairs reliably. By doing so, the network becomes capable of making inferences in mapping that is implied by the training data. This procedure involves minimizing a cost function. The cost function is often defined as the mismatch

between the network's mapping and the actual data.

A commonly used cost function is the mean-squared error between the average of network's output, f(x), and the target value y over all example pairs presented to the network. Minimizing this cost function in a gradient descent algorithm for a class of neural networks called Multi-Layer Perceptrons constitutes the basis of back-propagation algorithm (Demuth and Beale, 2002). In this study, we successfully developed and implemented a network with one hidden layers of 6 nodes.

Table 4. Dataset used for ANN.

Input Data		Output Data
Envelope Weighted Phase	Envelope Weighted Frequency	φ
0.224808	109.31568	0.1
-0.263106	91.767853	0.2
-0.565528	61.171856	0.3
-0.670387	57.455173	0.4
-0.675632	46.121319	0.5
0.323562	106.51822	0.1
-0.378417	83.861969	0.2
-0.56287	70.289696	0.3
-0.764093	51.647064	0.4
-0.663668	48.549095	0.5
0.409562	86.909805	0.1
-0.2364	91.413269	0.2
-0.496838	72.640099	0.3
-0.544338	64.44709	0.4
-0.785239	46.746338	0.5
0.488443	94.89753	0.1
-0.231116	93.647649	0.2
-0.437881	79.880699	0.3
-0.523854	67.820267	0.4
-0.74582	50.648357	0.5
0.574587	95.668144	0.1
-0.113229	98.605026	0.2
-0.456916	77.254433	0.3
-0.583435	66.380112	0.4
-0.715913	54.499546	0.5
0.61986	101.12841	0.1
-0.224508	96.966225	0.2
-0.365678	87.807404	0.3
-0.615403	68.697044	0.4
-0.675401	52.050041	0.5
0.727223	85.135704	0.1
-0.134636	100.91143	0.2
-0.346196	90.047951	0.3
-0.54664	71.183044	0.4
-0.658258	55.900189	0.5
0.732299	99.965302	0.1
-0.218339	96.199692	0.2
-0.33886	82.284752	0.3
-0.561999	63.738857	0.4
-0.816332	46.726818	0.5
0.6757	107.10917	0.1
-0.496571	84.066315	0.3
-0.38343	77.968796	0.4
-0.622469	59.316097	0.5

A dataset of 45 synthetic data points to train and test the neural network was used (Table 4). From this, 37 points (85% of the total data) were selected randomly for the network training and the remaining 30% of the data was used for testing the network. Each data point is a vector of two input values, namely, *EWP* and *EWF* as described earlier. The desired network output is synthetic *porosity* value. The input layer of the network receives input data at two nodes and the network generates an output at the final layer. We used the *Levenberg-Marquardt* (LM) method for training because it generally results in faster and more reliable convergence for our application.

The best and the worst results of 20 iterations for training of the network are presented in Table 5. In Table 5, RMS_{train} is the root-mean-square of the training error, and RMS_{test} is the root-mean-square of error during testing of the network. Considering the limited amount of data available for network training the results shown in Table 5 appear to be reasonable for practical applications. Other training algorithms such as Scaled conjugate gradient, One-Step Secant, and Fletcher-Powell Conjugate Gradient were also used but were discarded due to higher tolerance for the test errors and lower reliability in our application (Demuth and Beale, 2002). The results of the training are presented in Fig. 5.

Table 5. Error values for the best and the worst results.

RMS_{train}	RMS_{test}
0.03	0.03
0.05	0.06

In Fig. 5, R is the correlation coefficient between the real and the predicted porosity values; A being the predicated and T being the real value. The correlation coefficient is close to 1.0, implying a good network performance. The gap between values is caused by simulating data in special porosities (0.1, 0.2, ... , 0.5).

We used the abovementioned neural network for the task of classifying the test data. The results are shown in Fig. 6. During testing, a correlation coefficient of greater than 0.95 was generally obtained (as exhibited in Fig. 6). This shows that the porosity values in the test data were practically well-correlated with the network predictions. This is evident in Fig. 7 with the good performance of the trained network remarkably demonstrated for a set of synthetic test data. The real values of porosity, shown by small circles in Fig. 7 could be easily predicted by the back-propagating neural network, shown by small inverted triangles.

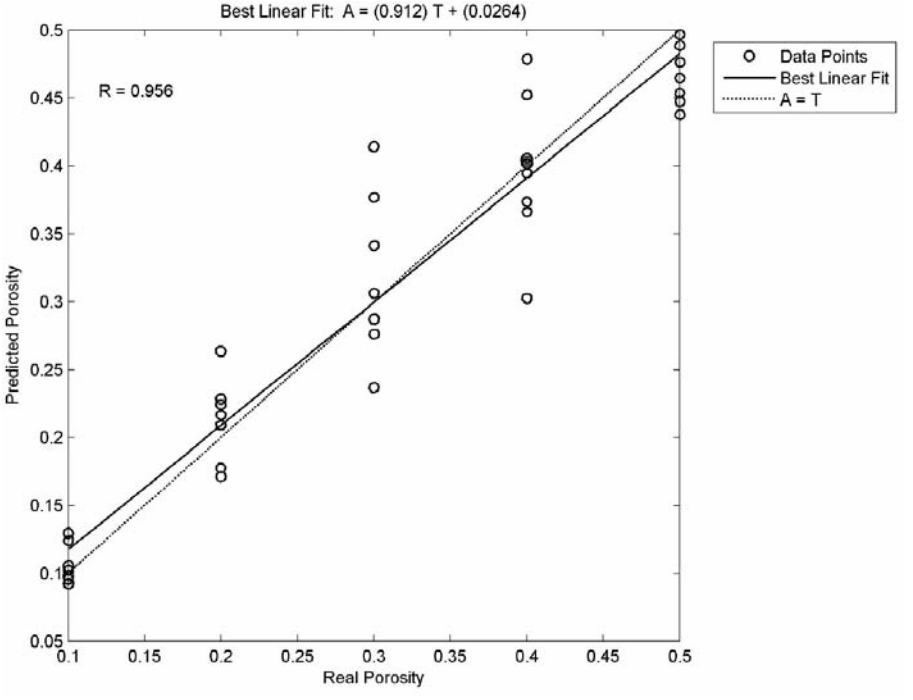

Fig. 5. Correlation coefficient for train data.

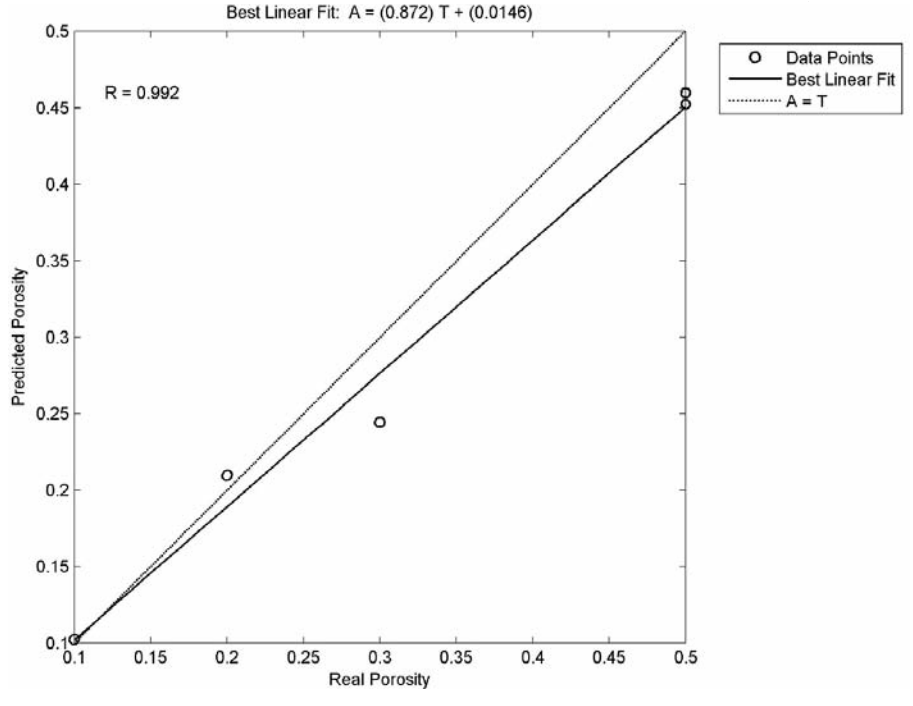

Fig. 6. Correlation coefficient for the test data.

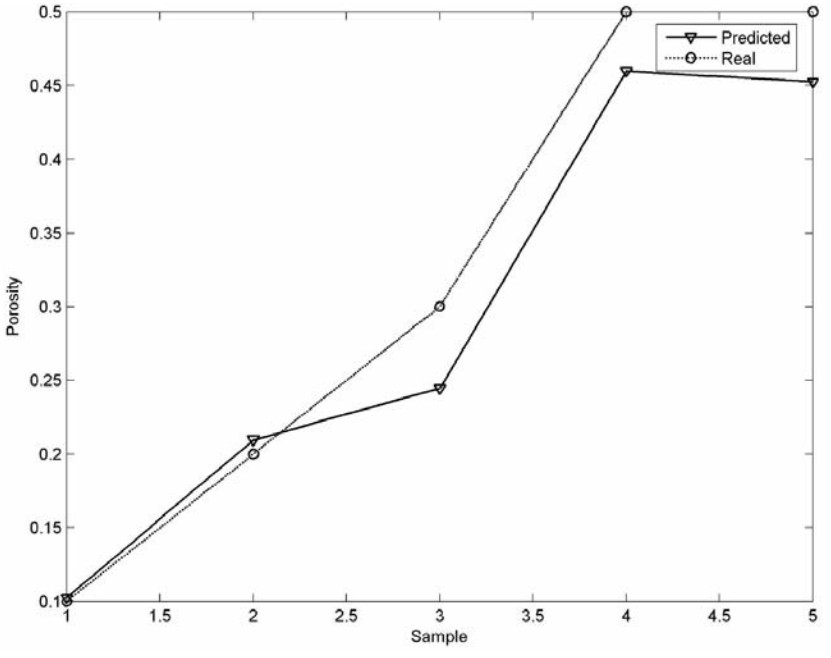

Fig. 7. Predicted results for a set of test data.

From Table 5, the reduction in the network error will increase the reliability of network's predictions, should additional training data be available or other method be used. In some cases, artificial neural networks detect the relative optimum point instead of global optimum point as a solution for the problem which is the main weak point for ANNs. Recognizing the computational power of support vector machines in rule generation and function approximation and their robustness particularly in the area of data classification, we embarked on development and training of a support vector regression machine (SVR) for the purpose of classification of porosities in this study.

Support Vector Machines (SVM) and their application for this study

In pattern recognition, the SVM algorithm constructs nonlinear decision functions by training a classifier to perform a linear separation in some high dimensional space which is nonlinearly related to input space. To generalize the SVM algorithm for regression analysis, an analogue of the margin is constructed in the space of the target values (y) by using Vapnik's ϑ-insensitive loss function (Fig. 8) (Quang-Anh et al., 2005).

$$|y - f(x)|_{\vartheta} = \max\{0, |y - f(x) - \vartheta|\} \quad . \tag{2}$$

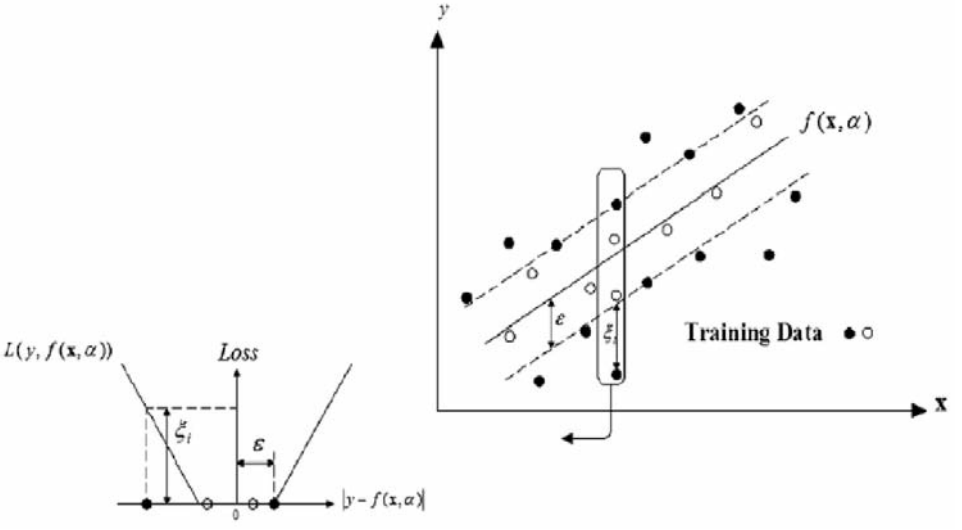

Fig. 8. Concept of e-insensitivity. Only the samples out of the $\pm\ \vartheta$-margin will have a non-zero slack variable, so they will be the only ones that will be part of the solution (Liu et al., 2009)

To estimate a linear regression

$$f(x) = (w \cdot x) + b \quad , \tag{3}$$

where w is the weighted matrix, x is the input vector and b is the bias term. With precision, one minimizes

$$\tfrac{1}{2} \| w \|^2 + C \sum_{i=1}^{m} |y - f(x)|_{\vartheta} \quad , \tag{4}$$

where C is a trade-off parameter to ensure the margin ϑ is maximized and error of the classification ξ is minimized. Considering a set of constraints, one may write the following relations as a constrained optimization problem:

$$L(w,\xi,\xi') = \tfrac{1}{2} \| w \|^2 + C \sum_{i=1}^{N} (\xi_i + \xi_i') \quad , \tag{5}$$

$$\text{subject to} \begin{cases} y_i - w^T \cdot x - b \leq \xi_i + \vartheta \quad , & (6) \\ w^T \cdot x + b - y_i \leq \xi_i' + \vartheta \quad , & (7) \\ \xi_i, \xi_i', x_i \geq 0 \quad . & (8) \end{cases}$$

That according to relations (6) and (7), any error smaller than ϑ does not require a non-zero ξ_i or ξ_i', and does not enter the objective function (2) (Lia et al., 2007).

By introducing Lagrange multipliers (α and α') and allowing for $C > 0$, $\vartheta > 0$ chosen a priori, the equation of an optimum hyper plane is achieved by maximizing of the following relations:

$$L(\alpha,\alpha') = \tfrac{1}{2} \sum_{i=1}^{N} \sum_{i=1}^{N} (\alpha_i - \alpha_i')x_i'x_i(\alpha_i - \alpha_i') + \sum_{i=1}^{N} [(\alpha_i - \alpha_i')y_i - (\alpha_i + \alpha_i')\vartheta \quad , \tag{9}$$

$$\text{subject to} \quad 0 \leq (\alpha_i - \alpha_i') \leq C \quad , \tag{10}$$

where x_i only appears inside an inner product. To get a potentially better representation of the data in non-linear case, the data points can be mapped into an alternative space, generally called feature space (a pre-Hilbert or inner product space) through a replacement:

$$x_i \cdot x_j \rightarrow \varphi(x_i) \cdot \varphi(x_j) \quad . \tag{11}$$

The functional form of the mapping $f(x_i)$ does not need to be known since it is implicitly defined by the choice of kernel: $k(x_i,x_j) = \varphi(x_i)\cdot\varphi(x_j)$ or inner product in Hilbert space. With a suitable choice of kernel the data can become separable in feature space while the original input space is still non-linear. Thus, whereas data for n-parity or the two spirals problem is non-separable by a hyper plane in input space, it can be separated in the feature space by the proper kernels. Table 6 gives some of the common kernels.

Table 6. Polynomial, normalized polynomial and Radial Basis Function (Gaussian) Kernels (Scholkopf et al., 1998).

Kernel Function	Type of Classifier
$K(x_i,x_j) = (x_i^T x_j + 1)^\rho$	Complete polynomial of degree ρ
$K(x_i,x_j) = (x_i^T x_j + 1)^\rho / \sqrt{\{(x_i^T x_j) - (y_i^T y_j)\}}$	Normalized polynomial kernel of degree ρ
$K(x_i,x_j) = \exp[\lVert (x_i - x_j) \rVert^2 / 2\sigma^2]$	Gaussian (RBF) with parameters σ which control the half-width of the curve fitting peak

Then, the nonlinear regression estimate takes the following form:

$$y_i = \sum_{i=1}^{N} \sum_{i=1}^{N} (\alpha_i - \alpha_i')\varphi(x_i)^T\varphi(x_j) + b = \sum_{i=1}^{N} \sum_{i=1}^{N} (\alpha_i - \alpha_i')K(x_i,x_j) + b \quad , (12)$$

where b is computed using the fact that eq. (6) becomes an equality with $\xi_i = 0$ if $0 < \alpha_i < C$, and relation (7) becomes an equality with $\xi_i' = 0$ if $0 < \alpha_i' < C$ (Chih-Hung et al., 2009).

Similar with other multivariate statistical models, the performances of SVM for regression depend on the combination of several parameters. They are capacity parameter C, ϑ of ϑ-insensitive loss function, the kernel type K and its corresponding parameters. C is a regularization parameter that controls the trade-off between maximizing the margin and minimizing the training error. In order to make the learning process stable, a large value should be set up for C (e.g., C = 100). The optimal value for ϑ depends on the type of noise present in the data, which is usually unknown. Even if enough knowledge of the noise is available to select an optimal value for ϑ, there is the practical consideration of the number of resulting support vectors. ϑ-insensitivity prevents the entire training set meeting boundary conditions, and so allows for the possibility of sparsity in the dual formulations solution. Therefore, choosing the appropriate value of ϑ is critical from theory.

Since in this study the nonlinear SVM is applied, it would be necessary to select a suitable kernel function. The obtained results of previous published researches indicate the Gaussian radial basis function has superior efficiency than other kernel functions (Wang et al., 2003). As it seen in the Table 6, the form of the Gaussian kernel is as follows:

$$K(x_i,x_j) = e^{-|x_i - x_j|^2/2\sigma^2} \quad . \quad (13)$$

In addition, where σ is a constant parameter of the kernel and can either control the amplitude of the Gaussian function and the generalization ability of SVM, we have to optimize σ and find the optimal one. In order to find the optimum values of two parameters (σ and ϑ) and prohibit the over-fitting of the model, the synthetic data set was separated into a training set (80% of available data for each borehole), a test set of 20% and the leave-one-out cross-validation of the whole training set was performed. The leave-one-out (LOO) procedure consists of removing one example from the training set, constructing the decision function on the basis only of the remaining training data and then testing on the removed example (Liu et al., 2006). In this fashion one tests all examples of the training data and measures the fraction of errors over the total number of training examples. The root mean square error (RMS) was used as an error function to evaluate the quality of model.

To obtain the optimal value of σ, the SVM with different σ were trained, the σ varying from 0.01 to 0.3, every 0.01. We calculated the RMS on different σ, according to the generalization ability of the model based on the LOO cross-validation for the training set in order to determine the optimal one. The optimal σ was found as 0.11. In order to find an optimal ϑ, the RMS on different ϑ was calculated. The optimal ϑ was found as 0.07. From the above discussion, the σ, ϑ and C were fixed at 0.11, 0.07 and 100, respectively. Fig. 9 is a schematic diagram showing the construction of the SVM.

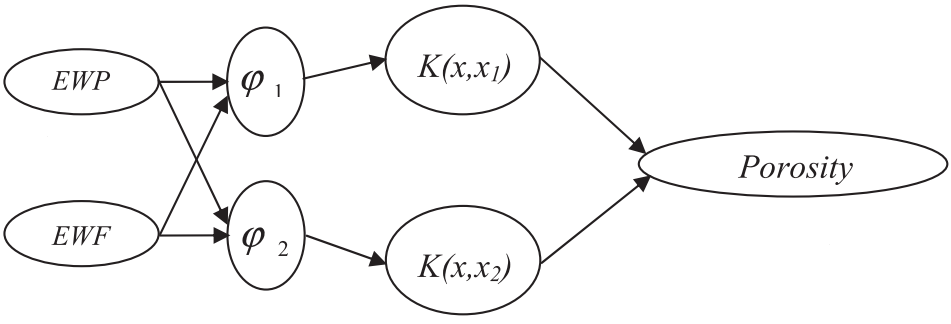

Fig. 9. schematic diagram of construction of the SVM.

The best and the worst results of 4 iterations for training of the network are presented in Table 7.

Table 7. Error values for the best and the worst results.

R_{train}	R_{test}	RMS_{train}	RMS_{test}
0.95	0.93	0.03	0.03
0.97	0.98	0.04	0.05

The results of the training are presented in Fig. 10.

As shown in Fig. 10 the correlation coefficient of training data is 0.96 implying the proper performance of SVM. The abovementioned support vector machine was used for the task of classifying the test data. The results are shown in Fig. 11. During testing, a correlation coefficient of greater than 0.95 was

generally obtained. This implies that the porosity values in the test data were practically well predicted using SVM. This is evident in Fig. 12 with the superior performance of the trained SVM remarkably demonstrated for a set of synthetic test data.

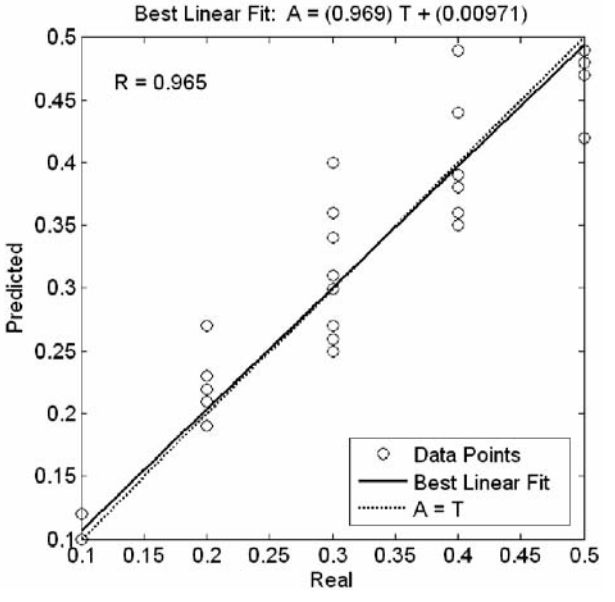

Fig. 10. Correlation coefficient for train data.

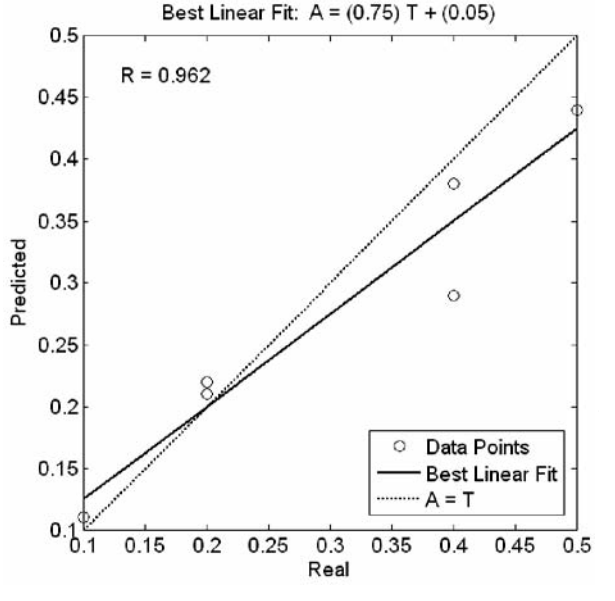

Fig. 11. Correlation coefficient for test data.

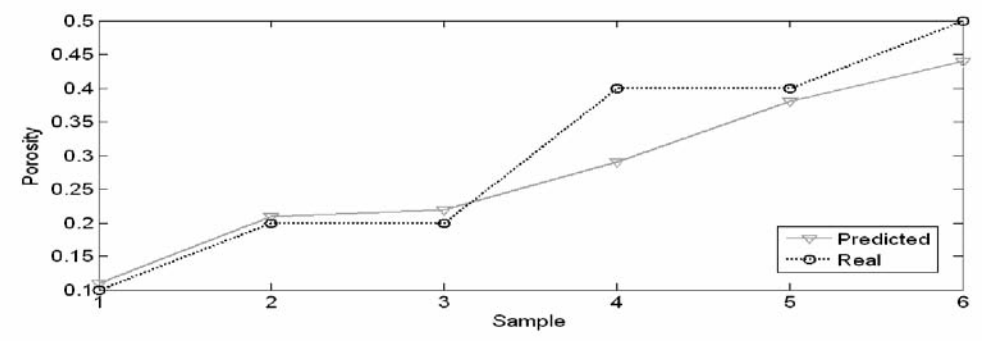

Fig. 12. Predicted results for a set of test data.

Application of the proposed ANN and SVM methods for real data of well 2

The results of previous chapters indicate that both BP and SVR methods could predict the values of porosity reliably for synthetic data. One of the major preferences of SVMs to ANNs is their superior performance facing little amounts of training data (Duda et al., 2002). Because of the small number of synthetic data in training process (37 data) and the differences between synthetic and real data (intricate and existence of noise in real data), it seems that BP can not be successfully implemented in predicting values of porosity for real data of well 2 using the previously trained model. Therefore the authors decided to use trained SVR for real porosity values prediction in this well.

To test the capability of the proposed methodology, data acquired from 3D seismic measurements in well 2 were used. The measurements were EWP and EWF (see Table 9).

Table 9. Data of well 2 used in trained SVR.

EWP	EWF	Porosity
0.55724	0.85255	0.14819
-1.2054	0.82066	0.10009
0.27508	0.79695	0.071772
1	0.80074	0.10006
-0.20119	0.7938	0.097834
-1.5889	0.89329	0.13987
-0.23435	1	0.14095
-1.1428	0.89089	0.13348
-1.4874	0.8068	0.15245

Fig. 13 shows the porosity values from the well log measurements (3rd column in Table 9) as real values and those obtained from support vector regression machine. For this test, the already trained SVR of synthetic data was used to make the prediction. The values of correlation coefficient and root mean square error of the prediction are 0.98 and 0.02, respectively. Fig. 13 exhibits a considerable coincidence between the results of support vector machine approach and that of well measurements.

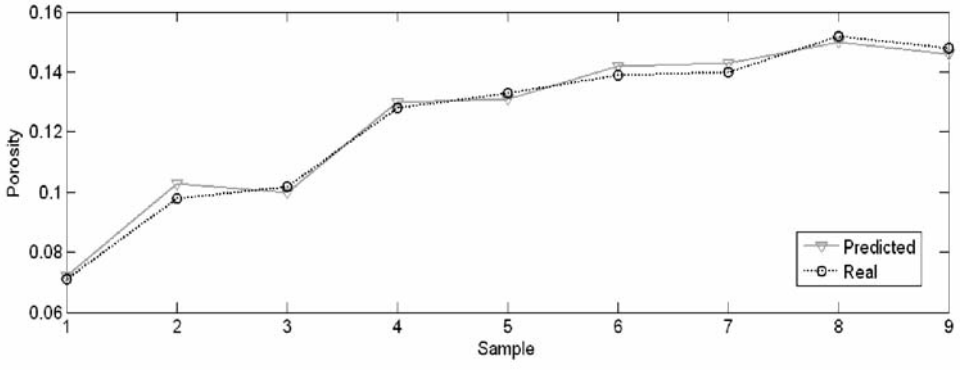

Fig. 13. Predicted results for a set of data in well 2.

CONCLUDING REMARKS

Measurement noise and nonlinear relationship between seismic data and porosity quantities exert difficulties in performing seismic data interpretation reliably. Consequently, other viable methods of prediction, such as the one proposed in this paper, may be deemed necessary in realistic cases. We successfully implemented and tested an artificial intelligent computational agent (a back-propagating neural network) and support vector regression machine (SVR) to consider the unknown nonlinear relationships between system variables in our prediction problem (foreseeing the porosity values) for synthetic data. Our approach uses envelope weighted phase and envelope weighted frequency as input system variables. The ANN and SVR seek the relationship between these input variables adaptively and strive to a desirable output which is, in our case, the values of porosity.

Synthetic data showed that both the ANN and SVR could train themselves very well with practically complete correlation between real porosity values and the predicted ones (correlation coefficient R of almost one). These methods also exhibited a remarkable capability in estimating the unknown zones (test data).

Since the number of synthetic data in training process is limited and according to the differences between synthetic and real data (intricate and existence of noise in real data), BP was not implemented in predicting values of porosity for real data of well 2 and only SVR was used for this purpose. Applying the machine to well 2 case while showing acceptable precision in prediction porosity; proved the performance of the machine. The SVR did predict the porosity values in well 2 reliably.

In this study, there was only an access to the data of well 2. To generalize the results of the abovementioned procedure, it is suggested to obtain sufficient reliable data samples from more wells in specific oil field and augmenting the training of the support vector machine with the new data. We speculate this would enhance the capability of the machine to use for the similar reservoirs.

ACKNOWLEDGMENT

The constructive comments and advice received during the course of this study from Dr. Iraj Abdollahi Fard of the National Iranian Oil Company is appreciated. The comments received from and the enlightening discussions with our anonymous reviewers improved the paper and are appreciated. The authors would also like to gratefully acknowledge the dGB Earth Sciences and the Exploration Directorate of the National Iranian Oil Company for their support of this project.

REFERENCES

Alimoradi, A., Moradzadeh, A. and Bakhtiari, M.R., 2011. Modifying Gassmann equation to determine the effect of pores sizes in carbonate reservoirs characterization. Petrol. Science, under review.

An, P., 1994. The effect of random noise in lateral reservoir characterization using feedforward neural networks. Expanded Abstr., 64th Ann. Internat. SEG Mtg., Los Angeles: 787-790.

An, P. and Moon, W.M., 1993. Reservoir characterization using feedforward neural networks. Expanded Abstr., 63rd Ann. Internat. SEG Mtg., Washington D.C.: 258-262.

An, P., Moon, W.M. and Kalantzis, F., 1997. Reservoir Property Estimation Using the Seismic Waveform and Feedforward Neural Networks. Report for Schlumberger.

Batyrshin, I., Kaynak, O. and Rudas, I., 2002. Fuzzy modeling based on generalized conjunction operations. IEEE Transact. Fuzzy Syst., 10: 678-683.

Batyrshin, I., Sheremetov, L., Markov, M. and Panova, A., 2005. Hybrid method for porosity classification in carbonate formations. J. Petrol. Science Engin., 47: 35-50.

Chih-Hung, W., Gwo-Hshiung, T. and Rong-Ho, L., 2009. A novel hybrid genetic algorithm for Kernel function and parameter optimization in support vector regression. Expert Syst. Applic., 36: 4725-4735.

Demuth, H. and Beale, M., 2002. Neural Network Toolbox for Use with MATLAB, Version 3.0, 742pp.

dGB Earth Sciences, 2008. Seismic Software & Services, OpendTect, Version 4.0

Duda, R.A., Hart, P.E. and Stork, D.G., 2002. Pattern Classification. Springer Verlag, Berlin.

Edalat, A. and Siahkoohi, H., 2007. Description of one of the Iranian hydrocarbon reservoirs using seismic facies analysis. Iran. Geophys. J., 11: 37-49.
Hagan, M.T., Demuth, H.B. and Beale, M., 1996. Neural Network Design. PWS Publishing Company, Boston, MA.
Jang, J.S.R., Sun, C.T. and Mizutani, E., 1997. Neuro-Fuzzy and Soft Computing: A Computational Approach to Learning and Machine Intelligence. Prentice Hall, Englewood Cliffs, NJ.
Lia, Q., Licheng, J. and Yingjuan, H., 2007. Adaptive simplification of solution for support vector machine. Pattern Recogn., 40: 972-980.
Lim, J.S., 2005. Reservoir properties determination using fuzzy logic and neural networks from well data in offshore Korea. J. Petrol. Sci. Engin., 49: 182-192.
Liu, H., Wen, S., Li, W., Xu, C. and Hu, C., 2009. Study on identification of oil/gas and water zones in geological logging based on support-vector machine. Fuzzy Inform. Engin., 2, AISC 62: 849-857.
Liu, H., Yao, X., Zhang, R., Liu, M., Hu, Z. and Fan, B., 2006. The accurate QSPR models to predict the bioconcentration factors of nonionic organic compounds based on the Heuristic method and support vector machine. Chemosphere, 63: 722-733.
Malvic, T. and Prskalo, S., 2007. Some benefits of the neural approach in porosity prediction case study from Benicanci Field. NAFTA, 58: 455-461.
Mavko, G., Mukerji, T. and Dvorkin, J., 2009. The Rock Physics Handbook. Cambridge University Press, Cambridge.
Mohaghegh, S., Arefi, R., Ameri, S., Amini, K. and Nutter, R., 1996. Petroleum reservoir characterization with the aid of artificial neural networks. J. Petrol. Sci. Engin., 16: 263-274.
Mohaghegh, S., Popa, A., Koperna, G. and Hill, D., 1999. Reducing the Cost of Field-Scale Log Analysis Using Virtual Intelligence Techniques. SPE 57454, Tulsa, OK.
Nikravesh, M., Aminzadeh, F. and Zadeh, L.A., 2003. Soft Computing and Intelligent Data Analysis. Elsevier Science Publishers, Amsterdam.
Pezeshk, S., Camp, C.V. and Karprapu, S., 1996. Geophysical log interpretation using neural network ASCE. J. Comput. Civil Engin., 10: 136-142.
Quang-Anh, T., Xing, L. and Haixin, D., 2005. Efficient performance estimate for one-class support vector machine. Pattern Recogn. Lett., 26: 1174-1182.
Raymer, L.L., Hunt, E.R. and Gardner, J.S., 1980. An improved sonic transit time-to-porosity transform. SPWLA Transact., 21st Ann. SPWLA Symp., Paper P, Tulsa, OK.
Scholkopf, B., Smola, A.J. and Muller, K.R., 1998. Nonlinear component analysis as a Kernel eigenvalues problem. Neural Comput., 10: 1299-1319.
Wang, W.J., Xu, Z.B., Lu, W.Z. and Zhang, X.Y., 2003. Determination of the spread parameter in the Gaussian Kernel for classification and regression. Neurocomput., 55: 643-663.
Wyllie, M.R.J., Gregory, A.R. and Gardner, L.W., 1958. An experimental investigation of factors affecting elastic wave velocities in porous media. Geophysics, 23: 459-493.